

# SEGIC: Unleashing the Emergent Correspondence for In-Context Segmentation

Lingchen Meng<sup>1,2</sup> Shiyi Lan<sup>3</sup> Hengduo Li<sup>4</sup> Jose M. Alvarez<sup>3</sup> Zuxuan Wu<sup>1,2†</sup> Yu-Gang Jiang<sup>1,2</sup>

<sup>1</sup>Shanghai Key Lab of Intell. Info. Processing, School of CS, Fudan University

<sup>2</sup>Shanghai Collaborative Innovation Center of Intelligent Visual Computing

<sup>3</sup>NVIDIA <sup>4</sup>University of Maryland

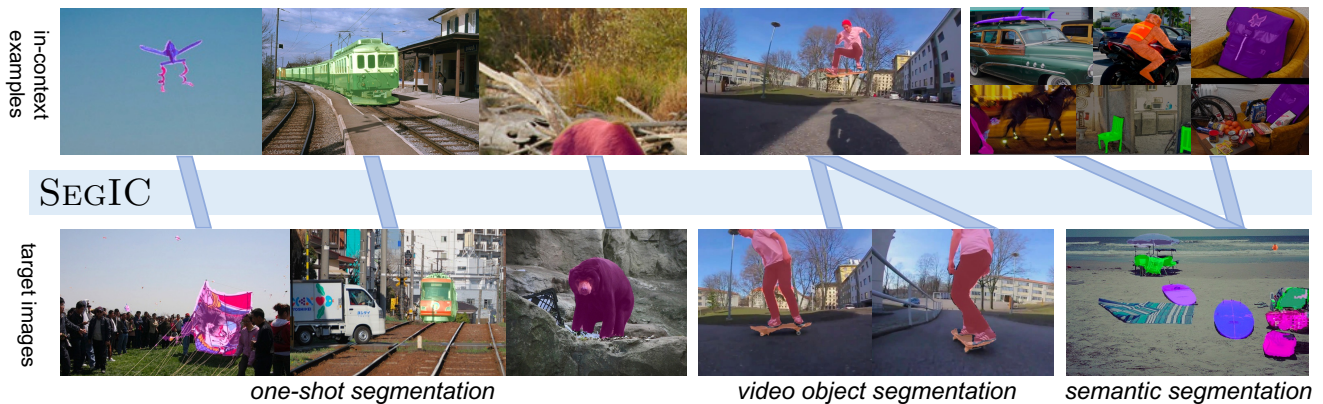



Figure 1. **Qualitative results of SEGIC.** SEGIC segments target images (the bottom row) according to a few labeled example images (top row, linked by  in the figure), termed as “in-context segmentation”. SEGIC unifies various segmentation tasks via different types of in-context samples, including the samples annotated with one mask per sample (one-shot segmentation), samples annotated with a few masks per sample (video object segmentation), and the combination of annotated samples (semantic segmentation)

## Abstract

*In-context segmentation aims at segmenting novel images using a few labeled example images, termed as “in-context examples”, exploring content similarities between examples and the target. The resulting models can be generalized seamlessly to novel segmentation tasks, significantly reducing the labeling and training costs compared with conventional pipelines. However, in-context segmentation is more challenging than classic ones due to its meta-learning nature, requiring the model to learn segmentation rules conditioned on a few samples, not just the segmentation. Unlike previous work with ad-hoc or non-end-to-end designs, we propose SEGIC, an end-to-end segment-in-context framework built upon a single vision foundation model (VFM). In particular, SEGIC leverages the emergent correspondence within VFM to capture dense relationships between target images and in-context samples. As such, information from in-context samples is then extracted into three types of instructions, i.e. geometric, visual, and meta instructions,*

*-serving as explicit conditions for the final mask prediction. SEGIC is a straightforward yet effective approach that yields state-of-the-art performance on one-shot segmentation benchmarks. Notably, SEGIC can be easily generalized to diverse tasks, including video object segmentation and open-vocabulary segmentation. Code will be available at <https://github.com/MengLcool/SEGIC>.*

## 1. Introduction

Modern advancements in deep learning have established a routine process for addressing visual perception challenges, typically involving data collection, model training, and deployment. While this pipeline is highly effective, it invariably demands additional effort in data acquisition and model tuning when adapting to new domains. Although researchers have been seeking to learn generic representations with pre-training, the resulting models have to be fine-tuned on the target domain for improved performance.

In contrast, the success of large language models (LLMs) [4, 46, 48, 49] in Natural Language Processing (NLP) offers an alternative approach. These models are trained on vast datasets, handling various NLP tasks

<sup>†</sup> Corresponding author.

through next-token prediction guided by prompts [46]. A key strength of LLMs is their ability to learn from a few examples, a process known as in-context learning (ICL). This enables them to adapt to various tasks with a small and varied set of instructions without requiring extensive fine-tuning or retraining [4, 46]. The success of ICL in NLP highlights the potential for applying similar strategies in visual perception tasks.

While appealing, ICL in vision is particularly challenging as vision tasks are significantly different regarding inputs (2D/3D), outputs (one-hot labels/bounding boxes), and specialized architectures. Recent advances in vision generalist models [29, 69, 70] suggest different levels of segmentation tasks, *i.e.* instance, semantic, and video, can be unified within the same output space. This motivates us to explore ICL using segmentation as a testbed and investigate whether current vision models can be easily generalized. While there are a few previous attempts on ICL for segmentation, they either have fallen short in performance due to implicit modeling [58, 59] or have employed heavy and non-end-to-end pipelines [35, 55, 66], which are less effective and efficient.

At the heart of ICL for NLP tasks is mining the relationships among different words and then propagating labels from a few task-specific question-answer pairs, namely in-context samples to the target one [1, 26, 61]. We argue that in vision tasks, the similar entity that facilitates label propagation from in-context samples to novel samples is establishing dense correspondences between images. Although dense visual correspondences are difficult to obtain before the era of foundation models, recent studies [6, 55] have shown that high-quality correspondence emerges in visual foundation models (VFMs) [6, 45, 50, 52].

In light of this, we introduce SEGIC, an end-to-end **segment-in-context** framework without the need for sophisticated handcrafted prompt design. Specifically, our framework is built upon a single frozen vision foundation model followed by a lightweight mask decoder. We leverage the emergent correspondence of the VFM to establish dense correspondences across target images and in-context samples. Based on that, we extract in-context information into three types of instructions: geometric, visual, and meta instructions. By explicitly utilizing these instructions, our model demonstrates remarkable generalization capabilities with low training costs across diverse segmentation tasks, as evidenced by extensive qualitative and quantitative experiments. We summarize our contributions in threefold:

- We introduce SEGIC, a simple yet effective in-context segmentation framework, exploring the strong emergent correspondence encoded in VFMs.
- We design geometric, visual, and meta instructions that explicitly transfer knowledge from in-context samples to the target to facilitate in-context segmentation.

- SEGIC demonstrates state-of-the-art performance on COCO-20<sup>i</sup>, FSS-1000 and recent LVIS-92<sup>i</sup>. Furthermore, SEGIC achieves competitive performance on novel tasks including video object segmentation and open-vocabulary segmentation, without ever seeing their training data.

## 2. Related Work

**Vision foundation models.** Recent years have witnessed great progress in large-scale vision pre-training [2, 6, 8, 16, 17, 25, 50], serving as the cornerstone for high-capacity foundation models. These pre-training approaches can be broadly categorized into two directions: vision-only pre-training [2, 6, 8, 16, 17, 45] and vision-language pre-training [21, 30, 50, 52, 64]. For vision-only pre-training, models aim to distinguish image/patch-level entities from different views [6, 8, 16] or reconstruct masked images [2, 16] from raw images. In vision-language pre-training, models strive to align cross-modal features into a unified visual-semantic space [21, 30, 50, 64], showcasing great open-set performance due to the transferable capabilities of language. Unlike these approaches that perform pre-training in an unsupervised or weakly supervised manner, SAM [25] is pre-trained on a huge amount of labeled segmentation data and can segment various entities with precise prompts about locations. In this paper, we conduct extensive experiments using three types of pre-trained models as backbones to explore their potential for in-context segmentation. Interestingly, we observe that models with higher zero-shot semantic and geometric correspondence performance are more likely to be effectively utilized in our SEGIC framework for in-context segmentation.

**Unified vision models.** Unified vision models have recently drawn significant attention due to their generalization capabilities and flexibilities. Unlike previous specialized vision models designed for specific datasets [7, 15, 36, 51, 60], vision generalists are tailored to handle multiple datasets [13, 39, 40, 68] and a wide range of tasks [20, 69, 70] within a single yet unified model. Recently, many studies [20, 25, 58, 59, 69, 70] have focused on developing techniques that unify segmentation tasks. In a similar spirit, our work also builds upon a unified output space for segmentation tasks. However, our goal is different—we aim to perform in-context segmentation that allows a model to effectively segment novel entities conditioned on a few samples.

**Visual correspondence.** Establishing visual correspondences between different images is vital for various computer vision tasks. Traditionally, computing correspondences is based on hand-designed features like SIFT [38] and SURF [3]. Deep models [23, 27, 57] can also learn correspondence in a supervised manner. More recently, it

has been shown features from large foundation models encode dense visual correspondence clues [2, 6, 16, 17, 45]. In this study, we discover a profound connection between correspondence and in-context segmentation—correspondence acts as explicit guidance, linking the target image with in-context images, thus facilitating label propagation for in-context segmentation.

**In-context learning.** For the first time, GPT-3 [4] introduces a new learning paradigm known as in-context learning, which unifies various NLP tasks as text completion or question-answering tasks using provided prompts and examples. This approach enables language models to handle various tasks, including novel ones, by leveraging task examples, without requiring re-training or fine-tuning. Recent studies [35, 58, 59] explore this mechanism in vision tasks. Painter [58] and SegGPT [59] aim to achieve in-context segmentation through in-painting. They build upon the Mask Image Modeling (MIM) framework [17] to concatenate images and predictions into a  $2 \times 2$  mosaic and make predictions by recovering the masked areas. In their pipelines, the vision backbone serves as both an image encoder and a mask decoder, which incurs significant computational costs. Moreover, they struggle to effectively leverage pre-trained models due to input shifts, leading to increased convergence challenges. Other approaches [35, 66] attempt using in-context segmentation via prompting SAM [25]. They build upon cross-image correspondences between in-context examples and target images by additional pre-trained models to generate prompts for SAM. However, these methods employ a two-stage pipeline, introducing redundancy and repeated computations. Consequently, if the model encounters limitations in one stage, it negatively impacts the final performance. In this work, we build an end-to-end in-context segmentation framework, leveraging the emergent correspondence using a single vision foundation model.

### 3. Approach

In-context learning equips a model with the ability to learn from example images, namely “in-context examples”, as humans, which has demonstrated great potential in NLP tasks [4, 46]. This process is akin to how humans intuitively grasp and replicate complex patterns from just a few guides, rapidly generalizing to new examples. In this paper, our goal is to establish an end-to-end in-context segmentation framework, enabling a model to effectively segment novel entities beyond the training set, such as video objects, with low training costs.

Formally, given a target image  $\mathbf{I} \in \mathbb{R}^{3 \times H \times W}$  where  $H$  and  $W$  represent the height and width, the goal is to segment a binary mask  $\mathbf{y} \in \mathbb{R}^{\{0,1\}^{H \times W}}$  conditioned on  $K$  in-context examples  $\{\mathbf{x}^r\}^K = \{(\mathbf{I}^r, \mathbf{y}^r)\}^K$ , where  $\mathbf{I}^r, \mathbf{y}^r$  are the image and ground-truth mask of an in-context example.

Our approach consists of four stages: feature extraction, correspondence discovery, in-context instruction extraction, and mask decoding, as shown in Figure 2. The feature extraction stage follows the common practice in visual perception tasks where we use a pre-trained visual foundation model to obtain the feature maps of both in-context and target images. Subsequently, we compute the dense correspondences based on their semantics and geometry (Section § 3.1), providing explicit guidance of the segmentation rules. Then, we extract in-context instructions based on the in-context samples and the dense correspondences (Section § 3.2). Finally, SEGIC uses a lightweight in-context mask decoder  $\mathcal{D}$  to produce segmentation masks for the desired target, leveraging the extracted information from in-context examples (Section § 3.3).

#### 3.1. Dense Correspondence Discovery

To establish the relations between the target image  $\mathbf{I}$  and the reference image  $\mathbf{I}^r$  (considering one reference example for brevity), we extract dense cross-image correspondences at the pixel level. For this purpose, we leverage pre-trained VFMs due to their powerful generalization capability and emergent correspondence properties. Specifically, we first extract the visual features of  $\mathbf{I}$  and  $\mathbf{I}^r$  with a vision foundation model, then apply the cosine distance function to compute the patch-level distance map between the two images as shown in Figure 2. We further obtain the pixel-level correspondences by interpolating the patch-level distance map to the size of the original image as follows:

$$\begin{aligned} \mathbf{f}, \mathbf{f}^r &= \mathcal{F}(\mathbf{I}), \mathcal{F}(\mathbf{I}^r) \\ \mathcal{C} &= \text{Upsample}(\text{Dist}(\mathbf{f}, \mathbf{f}^r)), \end{aligned} \quad (1)$$

where  $\mathcal{F}$  indicates the vision foundation model we use and  $\mathbf{f}, \mathbf{f}^r \in \mathbb{R}^{c \times h \times w}$  are the extracted features of the target and the reference images, respectively;  $c, h, w$  indicate the dimensions of the feature maps.  $\text{Dist}$  denotes the distance function (for which we use cosine distance) and  $\text{Upsample}$  is the interpolation function.  $\mathcal{C} \in \mathbb{R}^{HW \times HW}$  denotes the calculated dense correspondences between the target image and the in-context image.

#### 3.2. In-context Instruction Extraction

After obtaining dense correspondences, the question becomes how to utilize the in-context information, including in-context examples and dense correspondences, as instructions to guide the segmentation process. Here we extract in-context instructions based on ideas from NLP tasks [26, 46]. Ideally, the representation for in-context information should clearly articulate how segmentation should be executed on the target image while being concise and efficient for effective segmentation. To this end, we decouple and encode the in-context information into three individual in-context

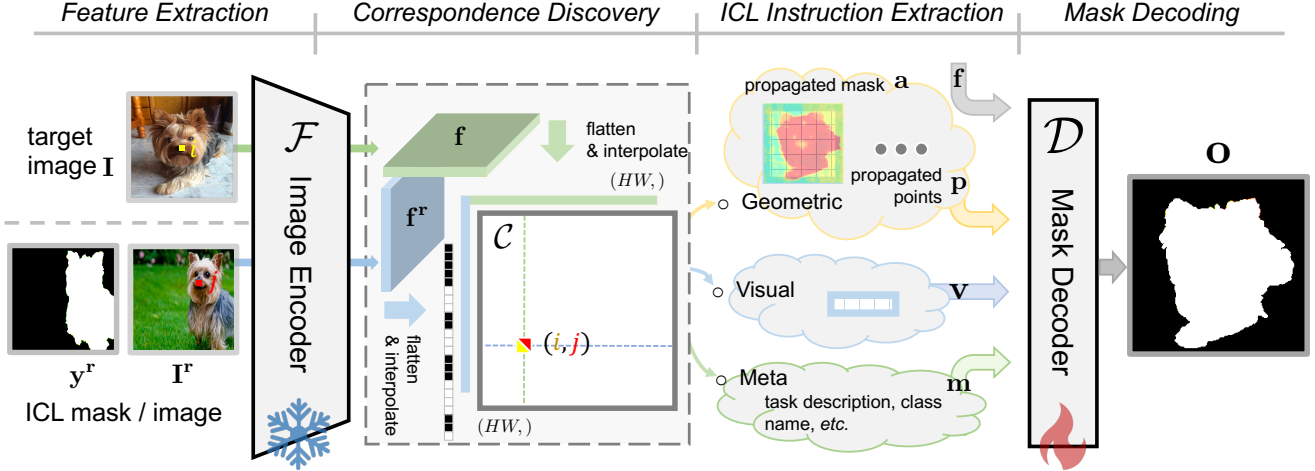


Figure 2. **Architecture overview.** SEGIC is built upon a frozen vision foundation model, consisting of four stages: (1) feature extraction; (2) correspondence discovery (Section § 3.1); (3) in-context instruction extraction (Section § 3.2); (4) mask decoding (Section § 3.3).

instructions as shown in Figure 2: 1) geometric instructions; 2) visual instructions; and 3) meta instructions, each of which will be elaborated below:

**Geometric instructions** aim to provide a coarse location estimation of the target mask. Although we only have the mask annotation for the reference image, we can propagate the label from the reference to the target to obtain a propagated mask by exploring the dense correspondences  $\mathcal{C}$ :

$$\begin{aligned} \mathbf{a} &= \mathbf{y}^r / \|\mathbf{y}^r\| \cdot \mathcal{C} \in \mathbb{R}^{H \times W} \\ \mathbf{p} &= \text{PE}(\text{Topk}(\mathbf{a})), \end{aligned} \quad (2)$$

where  $\mathbf{a}$  represents the propagated coarse mask for the target image. As shown in Equation (2), by performing matrix multiplication, we gather and average the dense correspondences based on the positive points in the reference mask. This process is analogous to propagating labels from the reference image to the target image through dense correspondences, making  $\mathbf{a}$  a form of dense geometric instruction. Additionally, based on  $\mathbf{a}$ , we employ Topk (as referred to in Equation (2)) to select the top-k points with the highest values in  $\mathbf{a}$ , indicating the locations most likely relevant to the target mask. We further encode the 2D coordinates into high-dimensional vectors using cosine positional encoding PE as in [54, 56], resulting in a type of sparse geometric instruction. Overall,  $\mathbf{a}$  and  $\mathbf{p}$  together provide geometric information extracted from in-context examples.

**Visual instructions** indicate the visual clues of the target entity. We use the mask label from the reference image to extract visual salient clues,  $\mathbf{v}$ , from reference features:

$$\mathbf{v} = \mathbf{y}^r / \|\mathbf{y}^r\| \cdot \mathbf{f}^r. \quad (3)$$

By doing so, only relevant information in reference features

as indicated in the mask, including low-level (texture, appearance, *etc.*) and high-level (semantics) clues, is used.

**Meta instructions** indicate other clues implicitly provided by in-context examples, such as task descriptions, class names, *etc.* We uniformly treat them as languages and encode them with a pre-trained language model, following [20, 25, 34].

$$\mathbf{m} = \mathcal{F}^t(\text{meta}) \quad (4)$$

where  $\mathcal{F}^t$  is the pre-trained CLIP text encoder [50], **meta** indicates the meta information and  $\mathbf{m}$  is the meta feature.

Finally, we use  $\mathbf{c} = \{\mathbf{a}, \mathbf{p}, \mathbf{v}, \mathbf{m}\}$  to denote the set of in-context instructions derived from reference samples, which can be further used for producing the segmentation mask, as will be introduced in section § 3.3.

### 3.3. Mask Decoding

In this section, we discuss how to predict the segmentation masks in target images following the aforementioned in-context instructions. In particular, we use a query-based mask decoder  $\mathcal{D}$  due to its high performance in segmentation tasks and flexibility [5, 9, 10]. Formally, the decoder network takes the target image feature  $\mathbf{f}$  and in-context instructions  $\mathbf{c}$  as input, as well as a learnable query  $\mathbf{q}$ , and outputs a mask  $\mathbf{o}$  as follows:

$$\mathbf{o} = \mathcal{D}(\mathbf{f}, \mathbf{c}; \mathbf{q}). \quad (5)$$

Unlike previous designs that use a set of object queries [5, 9, 10] for prediction, we only initialize one query since we just need to predict one mask in-context conditioned on the in-context instructions as shown in Figure 2.

To prepare these instructions for mask decoding, we first project them into the latent space used by the decoder. We



categorize the in-context instructions into two types according to their spatial property: instructions with spatial shapes (*i.e.* the propagated coarse mask  $\mathbf{a}$ ) and without spatial shapes (*i.e.*  $\mathbf{p}, \mathbf{v}, \mathbf{m}$ ). For the spatial instructions, we employ a series of convolutional layers  $\mathcal{M}$  to encode it into the image feature space; for the non-spatial instructions, we use projection layers  $\mathcal{P}$  to project them into the query feature space:

$$\begin{aligned} \mathbf{q}^{\mathbf{p}}, \mathbf{q}^{\mathbf{v}}, \mathbf{q}^{\mathbf{m}} &= \mathcal{P}^{\mathbf{p}}(\mathbf{p}), \mathcal{P}^{\mathbf{v}}(\mathbf{v}), \mathcal{P}^{\mathbf{m}}(\mathbf{m}) \\ \mathbf{a}' &= \mathcal{M}(\mathbf{a}) \end{aligned} \quad (6)$$

where  $\mathcal{P}^{\mathbf{p}}, \mathcal{P}^{\mathbf{v}}, \mathcal{P}^{\mathbf{m}}$  indicate the projection layers for  $\mathbf{p}, \mathbf{v}, \mathbf{m}$ , respectively.  $\mathbf{a}', \mathbf{q}^{\mathbf{p}}, \mathbf{q}^{\mathbf{v}}, \mathbf{q}^{\mathbf{m}}$  are the projected in-context instructions.

Furthermore, we inject the projected in-context instructions into the decoding stage to guide the decoder to segment in-context. Similarly, for the spatial features, we add them to image features, such that they are aware of the coarse mask produced by reference samples. For the non-spatial features, we concatenate the initial query with them, which allows a deeper interaction via a self-attention mechanism in the decoder:

$$\begin{aligned} \mathbf{f}' &= \mathbf{f} + \mathbf{a}' \\ \mathbf{q}' &= \text{Concat}(\mathbf{q}, \mathbf{q}^{\mathbf{l}}, \mathbf{q}^{\mathbf{s}}, \mathbf{q}^{\mathbf{m}}) \\ \mathbf{o} &= \mathcal{D}(\mathbf{f}'; \mathbf{q}') \end{aligned} \quad (7)$$

Finally, the mask prediction  $\mathbf{o}$  is produced based on image features  $\mathbf{f}'$  conditioned on instructions, and query features  $\mathbf{q}'$  as shown in Equation (7). For more details, please refer to our supplementary.

### 3.4. Training Pipeline

During training, we freeze all the parameters of the VFM and only leave the newly introduced mask decoder trainable. We employ a linear combination of a dice loss [53] and a binary cross-entropy loss for our mask loss:  $L_{mask} = \lambda_{ce}L_{ce} + \lambda_{dice}L_{dice}$ . It is worth noting that we calculate the segmentation loss on  $K$  selected points using importance sampling following [10, 24] instead of the whole image to save memory cost. To further improve the robustness toward noisy in-context samples, we introduce two strategies into our training recipe, namely ‘‘context reversion’’ and ‘‘negative entity augmentation’’.

**Context reversion.** We artificially introduce noisy context during training to improve the robustness. To simulate situations where in-context examples are inaccurate, we propose ‘‘context reversion’’: swapping the target and reference images—we use the prediction of the target image as an in-context example. The noisy context introduces randomness during training and hence can improve robustness.

**Negative entity augmentation.** In tasks like video object segmentation (VOS), in-context examples for different en-

tities in the same image are mutually exclusive. Taking the case of video object segmentation in Figure 1 as an example, the person and the skateboard are exclusive in one image. Thus, entities that are not of interest can serve as negative samples, indicating that they are not relevant to the target. We augment the in-context instructions with these negative entities for a better result.

## 4. Experiments

### 4.1. Training Data

We train SEGIC on semantic and instance segmentation datasets. Unlike previous sophisticated task-specific designs for multiple datasets/tasks, our method offers a simple approach that distinguishes tasks by in-context examples.

**COCO** [32] is a widely used instance/semantic segmentation with 83K training samples and 41K samples of 80 categories. We use the 2014 split version to be consistent with the COCO-20<sup>i</sup> one-shot semantic segmentation benchmark.

**ADE20k** [67] is a widely used semantic segmentation dataset for 150 categories, with 20K training images.

**LVIS** [14] is a large instance segmentation dataset containing 1000+ categories with  $\sim$ 100K training images.

### 4.2. Training Details

We implement SEGIC in PyTorch and use 8 V100 GPUs for most of our experiments. Thanks to the frozen backbone, our method is extremely memory-efficient (with less than 10G memory cost in most of our experiments). SEGIC is a single unified model that is jointly trained on mixed datasets, while evaluated on various datasets, separately. We utilize DINO-v2 [45] as the default vision foundation model, with a ViT-B for all ablations, and ViT-L/G for the main experiments. We employ an AdamW [37] optimizer with a weight decay of  $1e-4$ . We set an initial learning rate as  $1e-4$  and multiply 0.1 at the 10 epoch during training. Each dataset is sampled uniformly with 160K samples per epoch in the main experiments and 80K samples for the ablations. We perform dataset augmentations on target images and reference images respectively. We use large-scale jittering augmentation for semantic segmentation datasets, and normal data augmentations, including random resizing cropping, color jittering, and random horizontal flipping, for instance segmentation datasets. We random sample 1 mask per image for semantic segmentation datasets during training, while up to 10 masks for instance segmentation. The size of a single image is padded to  $896 \times 896$ .

### 4.3. Main Results

For the main experiments, we compare SEGIC with other specialist/generalist methods on several benchmarks. We

Method	<i>one-shot segmentation</i>			<i>video object segmentation</i>		<i>semantic seg</i>		<i>open-vocab seg</i>	
	COCO-20 <sup>i</sup> mean mIoU	FSS-1000 mIoU	LVIS-92 <sup>i</sup> mean mIoU	DAVIS-17 $\mathcal{J}\&\mathcal{F}$	YVOS-18 G	COCO mIoU	ADE20k mIoU	PC-459 mIoU	A-847 mIoU
<i>few-shot seg specialist</i>									
HSNet [42]	41.2/ 41.7	86.5	17.4	n/a	n/a	n/a	n/a	n/a	n/a
VAT [18]	41.3/ 42.9	90.3	18.5	n/a	n/a	n/a	n/a	n/a	n/a
FPTans [65]	47.0/ 56.5	-	-	n/a	n/a	n/a	n/a	n/a	n/a
<i>VOS specialist</i>									
AGAME [22]	n/a	n/a	n/a	70.0	66.0	n/a	n/a	n/a	n/a
SWEM [33]	n/a	n/a	n/a	84.3	82.8	n/a	n/a	n/a	n/a
XMem [11]	n/a	n/a	n/a	87.7	86.1	n/a	n/a	n/a	n/a
<i>semantic seg specialist</i>									
MaskFormer [9] (Swin-L)	n/a	n/a	n/a	n/a	n/a	64.8	54.1	n/a	n/a
Mask2Former [10] (Swin-L)	n/a	n/a	n/a	n/a	n/a	67.4	56.1	n/a	n/a
MaskDINO [28] (Swin-L)	n/a	n/a	n/a	n/a	n/a		56.6	n/a	n/a
<i>segmentation generalist</i>									
OneFormer [20] (Swin-L)	n/a	n/a	n/a	n/a	n/a	67.4	57.7	-	-
UNINEXT [63] (ViT-L)	n/a	n/a	n/a	77.2	78.1	-	-	-	-
X-decoder [69] (DaViT-L)	n/a	n/a	n/a	n/a	n/a	67.5	58.1	29.6	9.2
SEEM [70] (DaViT-L)	-	-	-	58.9	50.0	67.6	-	-	-
<i>in-context generalist</i>									
Painter [58] (MAE-L)	33.1	61.7	10.5	34.6	24.1	-	49.9	-	-
SegGPT [59] (MAE-L)	56.1	85.6	18.6	75.6	74.7	-	*39.6	-	-
PerSAM <sup>†‡</sup> [66] (SAM-G)	23.0	71.2	11.5	60.3	-	n/a	n/a	n/a	n/a
PerSAM-F <sup>†</sup> [25] (SAM-G)	23.5	75.6	12.3	71.9	-	n/a	n/a	n/a	n/a
Matcher <sup>†‡</sup> [35] (DINO-v2-G+SAM-G)	52.7	87.0	33.0	79.5	-	n/a	n/a	n/a	n/a
SEGIC <sup>†</sup> (DINO-v2-L)	76.1	86.8	44.6	71.4	62.7	#72.9	#55.5	#23.9	#14.8
SEGIC <sup>†</sup> (DINO-v2-G)	74.5	88.4	47.8	73.7	65.4	#74.0	#59.0	#24.0	#15.4

Table 1. **Main results on several segmentation benchmarks.** <sup>†</sup> indicates frozen image encoder; <sup>‡</sup> indicates training free method and using SAM; \* indicates that need additional fine-tuning, # indicates that classes within images are known during inference; n/a indicates the model does not have capability for the task and - indicates that do not have reported number.

use SEGIC of DINO-v2 [45] of large and giant versions as the backbone for the main experiments.

**One-shot semantic segmentation.** Following SegGPT [59], we have evaluated SEGIC in two one-shot semantic segmentation settings: in-domain using COCO-20<sup>i</sup> [43] (the training set of COCO-20<sup>i</sup> is a subset of ours) and out-of-domain with FSS-1000 [31] (without seeing any training samples of FSS-1000). As depicted in Table 1, SEGIC has achieved state-of-the-art performance in both of these settings. To ensure a fair comparison, we report both out-of-domain (the former) and in-domain (the latter) performance of specialist models for COCO-20<sup>i</sup>, split by / in Table 1. Additionally, for FSS-1000, we highlight the performance trained on FSS-1000 in gray and zero-shot results in black. Notably, SEGIC outperforms previous generalist models by a significant margin (more than 20 of mean mIoU) on COCO-20<sup>i</sup> and achieves competitive results that are very close to specialist models on FSS-1000, even without ever being trained on it. Furthermore, we conduct experiments on LVIS-92<sup>i</sup> [35], a more challenging one-shot benchmark built upon LVIS [14]. On LVIS-92<sup>i</sup>, SEGIC surpasses Matcher, the previous best model, by a large margin (from 33.0 to 47.8).

Since we include the evaluation categories in the training process for COCO-20<sup>i</sup> in Table 1, for a rigorous comparison, we follow its training setting that trains and tests

Method	F0	F1	F2	F3	mean
HSNet [42]	37.2	44.1	42.4	41.3	41.2
VAT [18]	39.0	43.8	42.6	39.7	41.3
FPTans [65]	44.4	48.9	50.6	44.0	47.0
MSANet [19]	47.8	57.4	48.7	50.5	51.1
SEGIC	55.8	54.7	52.4	51.4	53.6
SEGIC <sup>‡</sup>	<b>62.3</b>	<b>62.5</b>	<b>63.3</b>	<b>60.9</b>	<b>62.3</b>

Table 2. **Comparisons on one-shot COCO-20<sup>i</sup>.** <sup>‡</sup> indicates that the model is jointly trained on the COCO-excluded datasets.

our model on 4 splits [43] separately, avoiding seeing categories for evaluation. As shown in Table 2, our method still achieves state-of-the-art performance on COCO-20<sup>i</sup>. Furthermore, as shown in the last row of Table 2, by joint training on COCO-excluded datasets (including ADE20k, LVIS, and FSS-1000), there is a significant performance gain across all splits. This further demonstrates the effectiveness of our in-context generalization capabilities.

Overall, our best model surpasses all previous segmentation generalist models across all one-shot segmentation benchmarks, demonstrating its effectiveness.

**Zero-shot video object segmentation.** Video object segmentation (VOS) aims to segment specific objects in video frames. In this work, we focus on the semi-supervised VOS

setting, where the masks that appeared first time are given as references. We evaluate SEGIC on the validation set of two commonly used VOS datasets: DAVIS-17 [47] and YouTube-VOS-18 [62]. We export two metrics commonly used in VOS for evaluation: the  $\mathcal{J}\&\mathcal{F}$  score for DAVIS-17 and  $G$  score for YouTube-VOS-18, with their official evaluation servers or toolkits. As shown in Table 1, when compared to VOS specialist models, SEGIC achieves competitive performance on VOS benchmarks, even without seeing any training videos. Furthermore, in comparison to segmentation generalist models, SEGIC surpasses Painter [58], SEEM [70], and PerSAM [66] by a significant margin, and competes favorably with recent generalist models [35, 59]. Additionally, the VOS task pipeline in SEGIC is relatively simple. We do not use any test time augmentation tricks (TTA) used in [11]. Moreover, it does not involve dense feature interaction at the patch level, as in SegGPT, and does not require the use of a pre-trained SAM for segmentation.

**Generic semantic segmentation.** We also evaluate SEGIC on generic semantic segmentation. We use two widely-used semantic segmentation datasets, COCO [32] and ADE20k [67], for evaluation. To meet our in-context learning framework, we initially gather in-context examples from the training set along with the classes within each image and then perform segmentation in an in-context manner. As illustrated in Table 1, compared to specialist and generalist models for semantic segmentation, SEGIC demonstrates strong performance under the settings that the classes are known in advance (marked with #). As shown in Table 1, our best model achieves 74.0 and 59.0 mIoU on COCO and ADE20k, respectively, surpassing the previous specialist and generalist models.

**Open-vocabulary semantic segmentation.** Similar to generic semantic segmentation, we can also extend SEGIC to open-vocabulary semantic segmentation with the assistance of diffusion models. We employ in-context examples like one-shot segmentation to provide in-context examples for novel categories. Furthermore, we could also utilize StableDiffusion [52] to synthesize in-context examples like [44]. Compared to X-decoder [69], our method obtains competitive results on PC-459 and even outperforms previous methods on ADE-847.

#### 4.4. Ablation Study

In the ablation study, we report the performance on COCO-20<sup>i</sup> (in-domain one-shot segmentation), FSS-1000 (out-of-domain one-shot segmentation) and DAVIS-17 (zero-shot video object segmentation) to investigate the in-domain convergence and out-of-domain generalization capability.

**Different vision foundation models.** We further investigate the potential of each pre-trained VFM for in-context segmentation, including DINO-v1/v2 [6, 45],

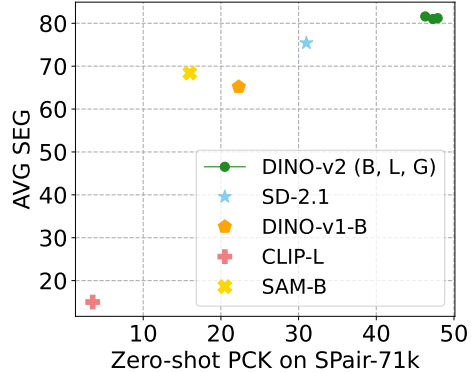


Figure 3. **Performance between semantic correspondence and segmentation.** We directly use the dense correspondences to zero-shot perform flow estimation for PCK.

SAM-encoder [25], StableDiffusion-2.1 (SD-2.1) [52, 55], and CLIP [50]. For each VFM, we freeze it to extract image features and dense correspondences then map them into the latent space for mask decoding, equally. As shown in Table 3a, the vision-language pre-trained model, CLIP, only achieves trivial performance on three datasets. This indicates that features learned by image-level vision-language alignment cannot be directly applied to fine-grained segmentation without fine-tuning. Additionally, its low-resolution pre-training may also contribute to poor performance. Meanwhile, other VLMs (*i.e.* DINO-v1/v2, SAM image encoder, and StableDiffusion) achieve decent performance on the segmentation benchmarks. Specifically, for StableDiffusion, we follow the usage in [52] to extract image features with 1-step diffusion. It is worth noting that the DINO-v2 series achieves the best performance, even outperforming the encoder of SAM, which is pre-trained for segmentation. We attribute this to its use of advanced vision contrastive learning as its pretext task, which learns the relation between different views within/across images, most relevant to dense correspondence. Besides, pre-training with high resolutions, *e.g.* DINO-v2, SD-2.1, may also help the segmentation. This implies that if the pretext task of a VFM is close to dense correspondence, this model is more likely to be easily extended into an in-context segmentation model.

**Relation between correspondence and segmentation.** We further conduct an experiment to study the relationship between correspondence and segmentation performance with different backbones. We evaluate a percent of correct keypoints score (PCK) on SPair-71k [41] following to [12], as well as the average segmentation score among COCO-20<sup>i</sup>, FSS-1000, and DAVIS-17. As shown in Figure 3, the performance on segmentation is proportional to correspondence, demonstrating a strong consistency between these two tasks. It further confirms our motivation that leverage

Encoder	COCO-20 <sup>i</sup>	FSS-1000	DAVIS-17
DINO-v2-B [45]	74.6	87.4	70.1
DINO-v2-L [45]	75.4	86.9	68.9
DINO-v2-G [45]	75.7	87.5	70.1
SAM-B [25]	59.8	76.9	60.1
DINO-v1-B [6]	53.5	76.9	54.2
SD-2.1 [52]	66.6	84.2	52.4
CLIP-L [50]	15.0	30.4	3.0

(a) **Ablation on foundation models as encoder.**

■ means that we only obtain a trivial performance.

reversion negative	COCO-20 <sup>i</sup>	FSS-1000	DAVIS-17
	70.0	86.1	66.3
✓	72.9	86.9	65.0
✓	73.1	86.5	64.3
✓ ✓	<b>74.6</b>	<b>87.3</b>	<b>70.1</b>

(c) **Ablations the training strategies.** reversion and negative indicate context reversion and negative entity augmentation, respectively. ■ is the default training scheme in our main experiments.

geometric	visual	meta	COCO-20 <sup>i</sup>	FSS-1000	DAVIS-17
✓			68.8	87.3	65.8
	✓		71.0	85.1	67.6
		✓	73.7	63.7	21.6
			48.9	58.1	21.1
✓	✓	✓	<b>74.6</b>	<b>87.4</b>	<b>70.1</b>

(b) **Component ablation on in-context instructions.** Geometric, visual, and meta indicate the corresponding in-context instructions, respectively. ■ is the default setting for in-context instructions in the main experiment.

semantic segmentation		instance segmentation		COCO-20 <sup>i</sup>	FSS-1000	DAVIS-17	AVG
COCO <sub>sem</sub>	ADE20k	COCO <sub>inst</sub>	LVIS				
✓				<b>76.3</b>	80.9	45.1	67.4
✓	✓			75.6	82.3	40.1	66.0
✓		✓		75.7	83.5	<b>70.1</b>	76.4
✓	✓	✓	✓	74.6	<b>87.4</b>	68.4	<b>76.8</b>

(d) **Ablations on training data.** COCO<sub>sem</sub> and COCO<sub>inst</sub> indicate that we treat COCO annotation as semantic and instance segmentation, respectively. AVG indicates the average score among all three benchmarks. ■ is the default data combination in our main experiments.

Table 3. **SEGIC ablations.** We report mean mIoU for COCO-20<sup>i</sup>, mIoU for FSS-1000 and  $\mathcal{J}\&\mathcal{F}$  score for DAVIS-17 in all ablations.

the emergent correspondence for in-context segmentation.

**Ablations on in-context instructions.** We study the importance of each component of in-context instructions (*i.e.* geometric, visual, and meta instructions). We conduct ablations on different combinations of components. As shown in Table 3b, we find that the geometric and visual instructions tend to help the performance for out-of-domain segmentation and meta instructions (class name and task description in the ablation) benefit in-domain performance: when each component is used individually, the geometric and visual instructions obtain the best results on FSS-1000 and DAVIS-17, respectively. Meanwhile, meta instructions achieve the best performance on COCO-20<sup>i</sup>, but with poor results on the other two datasets. Encouragingly, our method obtains the best performance among three tasks when using all three prompts, further demonstrating that our model can effectively transfer knowledge from in-context samples with the proposed in-context instructions.

**Ablations on training strategies.** We investigate how the proposed training strategies affect performance. As shown in Table 3c, since the two strategies, *i.e.* context reversion and negative entity augmentation, act as a form of “in-context augmentation”, they bring performance gains on COCO-20<sup>i</sup> and FSS-1000<sup>i</sup>. However, the performance slightly drops on DAVIS-17. Furthermore, after combining them, our model achieves a consistent gain across all datasets, highlighting its efficacy.

**Dataset Combination.** We further investigate the effectiveness of each dataset under our joint in-context train-

ing framework. We group the training data into two types: semantic segmentation (COCO<sub>sem</sub>, ADE20k) and instance segmentation (COCO<sub>inst</sub>, LVIS). As shown in Table 3d, it is clear to see that when trained on COCO<sub>sem</sub> only, it achieves the best performance on COCO-20<sup>i</sup> with a weak performance on FSS-1000 and DAVIS-17. Based on this, we can enrich the training data from two directions: (1) use extra semantic segmentation data and (2) introduce instance segmentation tasks into training. For the former direction, after introducing ADE20k into training, the performance on FSS-1000 increases with little performance drop on the other two datasets. For the latter, we still use COCO as the training set but introduce instance segmentation with its instance-level annotation. It can be seen a clear performance boost of more than 20 points of  $\mathcal{J}\&\mathcal{F}$  score (45.1→70.1) on DAVIS-17, since video object segmentation needs an instance-level understanding. Finally, we further enrich our training data with LVIS [14], and our model achieves the most balanced performance among the three datasets.

## 5. Conclusion

We introduced SEGIC, an end-to-end in-context segmentation framework that leverages the emergent correspondence of a single frozen vision foundation model. By training on standard segmentation datasets, SEGIC achieved state-of-the-art performance on one-shot segmentation benchmarks, including COCO-20<sup>i</sup>, FSS-1000, and LVIS-92<sup>i</sup>. Impressively, SEGIC demonstrated competitive performance on novel tasks, providing a cost-effective training approach for universal segmentation. In this work, our primary focus is



on utilizing one in-context example per entity. In the future, we plan to explore utilizing multiple in-context examples to enhance contextual information. Additionally, we aim to investigate our model’s potential in instance-level segmentation, such as open-world instance segmentation. We do not anticipate any undesirable ethical or social impacts.

**Acknowledgement** We would like to express our appreciation for the valuable discussion with Xinlong Wang.

## References

- [1] Ivana Balažević, David Steiner, Nikhil Parthasarathy, Relja Arandjelović, and Olivier J Hénaff. Towards in-context scene understanding. *arXiv preprint arXiv:2306.01667*, 2023.
- [2] Hangbo Bao, Li Dong, Songhao Piao, and Furu Wei. Beit: Bert pre-training of image transformers. In *ICLR*, 2021.
- [3] Herbert Bay, Tinne Tuytelaars, and Luc Van Gool. Surf: Speeded up robust features. In *ECCV*, 2006.
- [4] Tom Brown, Benjamin Mann, Nick Ryder, Melanie Subbiah, Jared D Kaplan, Prafulla Dhariwal, Arvind Neelakantan, Pranav Shyam, Girish Sastry, Amanda Askell, et al. Language models are few-shot learners. In *NeurIPS*, 2020.
- [5] Nicolas Carion, Francisco Massa, Gabriel Synnaeve, Nicolas Usunier, Alexander Kirillov, and Sergey Zagoruyko. End-to-end object detection with transformers. In *ECCV*, 2020.
- [6] Mathilde Caron, Hugo Touvron, Ishan Misra, Hervé Jégou, Julien Mairal, Piotr Bojanowski, and Armand Joulin. Emerging properties in self-supervised vision transformers. In *ICCV*, 2021.
- [7] Liang-Chieh Chen, George Papandreou, Iasonas Kokkinos, Kevin Murphy, and Alan L Yuille. Deeplab: Semantic image segmentation with deep convolutional nets, atrous convolution, and fully connected crfs. *TPAMI*, 2017.
- [8] Ting Chen, Simon Kornblith, Mohammad Norouzi, and Geoffrey Hinton. A simple framework for contrastive learning of visual representations. In *ICML*, 2020.
- [9] Bowen Cheng, Alex Schwing, and Alexander Kirillov. Per-pixel classification is not all you need for semantic segmentation. In *NeurIPS*, 2021.
- [10] Bowen Cheng, Ishan Misra, Alexander G Schwing, Alexander Kirillov, and Rohit Girdhar. Masked-attention mask transformer for universal image segmentation. In *CVPR*, 2022.
- [11] Ho Kei Cheng and Alexander G Schwing. Xmem: Long-term video object segmentation with an atkinson-shiffrin memory model. In *ECCV*, 2022.
- [12] Seokju Cho, Sunghwan Hong, and Seungryong Kim. Cats++: Boosting cost aggregation with convolutions and transformers. *TPAMI*, 2022.
- [13] Xiuye Gu, Yin Cui, Jonathan Huang, Abdullah Rashwan, Xuan Yang, Xingyi Zhou, Golnaz Ghiasi, Weicheng Kuo, Huizhong Chen, Liang-Chieh Chen, et al. Dataseg: Taming a universal multi-dataset multi-task segmentation model. *arXiv preprint arXiv:2306.01736*, 2023.
- [14] Agrim Gupta, Piotr Dollár, and Ross Girshick. Lvis: A dataset for large vocabulary instance segmentation. In *CVPR*, 2019.
- [15] Kaiming He, Georgia Gkioxari, Piotr Dollár, and Ross Girshick. Mask r-cnn. In *ICCV*, 2017.
- [16] Kaiming He, Haoqi Fan, Yuxin Wu, Saining Xie, and Ross Girshick. Momentum contrast for unsupervised visual representation learning. In *CVPR*, 2020.
- [17] Kaiming He, Xinlei Chen, Saining Xie, Yanghao Li, Piotr Dollár, and Ross Girshick. Masked autoencoders are scalable vision learners. In *CVPR*, 2022.
- [18] Sunghwan Hong, Seokju Cho, Jisu Nam, Stephen Lin, and Seungryong Kim. Cost aggregation with 4d convolutional swin transformer for few-shot segmentation. In *ECCV*, 2022.
- [19] Ehtesham Iqbal, Sirojbek Safarov, and Seongdeok Bang. Msanet: Multi-similarity and attention guidance for boosting few-shot segmentation. *arXiv preprint arXiv:2206.09667*, 2022.
- [20] Jitesh Jain, Jiachen Li, Mang Tik Chiu, Ali Hassani, Nikita Orlov, and Humphrey Shi. Oneformer: One transformer to rule universal image segmentation. In *CVPR*, 2023.
- [21] Chao Jia, Yinfei Yang, Ye Xia, Yi-Ting Chen, Zarana Parekh, Hieu Pham, Quoc Le, Yun-Hsuan Sung, Zhen Li, and Tom Duerig. Scaling up visual and vision-language representation learning with noisy text supervision. In *ICML*, 2021.
- [22] Joakim Johlander, Martin Danelljan, Emil Brissman, Fahad Shahbaz Khan, and Michael Felsberg. A generative appearance model for end-to-end video object segmentation. In *CVPR*, 2019.
- [23] Seungwook Kim, Juhong Min, and Minsu Cho. Transformer: Match-to-match attention for semantic correspondence. In *CVPR*, 2022.
- [24] Alexander Kirillov, Yuxin Wu, Kaiming He, and Ross Girshick. Pointrend: Image segmentation as rendering. In *CVPR*, 2020.
- [25] Alexander Kirillov, Eric Mintun, Nikhila Ravi, Hanzi Mao, Chloe Rolland, Laura Gustafson, Tete Xiao, Spencer Whitehead, Alexander C Berg, Wan-Yen Lo, et al. Segment anything. *arXiv preprint arXiv:2304.02643*, 2023.
- [26] Jannik Kossen, Tom Rainforth, and Yarin Gal. In-context learning in large language models learns label relationships but is not conventional learning. *arXiv preprint arXiv:2307.12375*, 2023.
- [27] Jae Yong Lee, Joseph DeGol, Victor Fragoso, and Sudipta N Sinha. Patchmatch-based neighborhood consensus for semantic correspondence. In *CVPR*, 2021.
- [28] Feng Li, Hao Zhang, Huaizhe Xu, Shilong Liu, Lei Zhang, Lionel M Ni, and Heung-Yeung Shum. Mask dino: Towards a unified transformer-based framework for object detection and segmentation. In *CVPR*, 2023.
- [29] Hao Li, Jinguo Zhu, Xiaohu Jiang, Xizhou Zhu, Hongsheng Li, Chun Yuan, Xiaohua Wang, Yu Qiao, Xiaogang Wang, Wenhui Wang, et al. Uni-perceiver v2: A generalist model for large-scale vision and vision-language tasks. In *CVPR*, 2023.
- [30] Junnan Li, Ramprasaath Selvaraju, Akhilesh Gotmare, Shafiq Joty, Caiming Xiong, and Steven Chu Hong Hoi. Align before fuse: Vision and language representation learning with momentum distillation. In *NeurIPS*, 2021.

- [31] Xiang Li, Tianhan Wei, Yau Pun Chen, Yu-Wing Tai, and Chi-Keung Tang. Fss-1000: A 1000-class dataset for few-shot segmentation. In *CVPR*, 2020.
- [32] Tsung-Yi Lin, Michael Maire, Serge Belongie, James Hays, Pietro Perona, Deva Ramanan, Piotr Dollár, and C Lawrence Zitnick. Microsoft coco: Common objects in context. In *ECCV*, 2014.
- [33] Zhihui Lin, Tianyu Yang, Maomao Li, Ziyu Wang, Chun Yuan, Wenhao Jiang, and Wei Liu. Swem: Towards real-time video object segmentation with sequential weighted expectation-maximization. In *CVPR*, 2022.
- [34] Shilong Liu, Zhaoyang Zeng, Tianhe Ren, Feng Li, Hao Zhang, Jie Yang, Chunyuan Li, Jianwei Yang, Hang Su, Jun Zhu, et al. Grounding dino: Marrying dino with grounded pre-training for open-set object detection. *arXiv preprint arXiv:2303.05499*, 2023.
- [35] Yang Liu, Muzhi Zhu, Hengtao Li, Hao Chen, Xinlong Wang, and Chunhua Shen. Matcher: Segment anything with one shot using all-purpose feature matching. *arXiv preprint arXiv:2305.13310*, 2023.
- [36] Jonathan Long, Evan Shelhamer, and Trevor Darrell. Fully convolutional networks for semantic segmentation. In *CVPR*, 2015.
- [37] Ilya Loshchilov and Frank Hutter. Decoupled weight decay regularization. *arXiv preprint arXiv:1711.05101*, 2017.
- [38] David G Lowe. Distinctive image features from scale-invariant keypoints. *IJCV*, 2004.
- [39] Lingchen Meng, Xiyang Dai, Yinpeng Chen, Pengchuan Zhang, Dongdong Chen, Mengchen Liu, Jianfeng Wang, Zuxuan Wu, Lu Yuan, and Yu-Gang Jiang. Detection hub: Unifying object detection datasets via query adaptation on language embedding. In *CVPR*, 2023.
- [40] Lingchen Meng, Xiyang Dai, Jianwei Yang, Dongdong Chen, Yinpeng Chen, Mengchen Liu, Yi-Ling Chen, Zuxuan Wu, Lu Yuan, and Yu-Gang Jiang. Learning from rich semantics and coarse locations for long-tailed object detection. *arXiv preprint arXiv:2310.12152*, 2023.
- [41] Juhong Min, Jongmin Lee, Jean Ponce, and Minsu Cho. Spair-71k: A large-scale benchmark for semantic correspondence. *arXiv preprint arXiv:1908.10543*, 2019.
- [42] Juhong Min, Dahyun Kang, and Minsu Cho. Hypercorrelation squeeze for few-shot segmentation. In *CVPR*, 2021.
- [43] Khoi Nguyen and Sinisa Todorovic. Feature weighting and boosting for few-shot segmentation. In *CVPR*, 2019.
- [44] Quang Ho Nguyen, Truong Tuan Vu, Anh Tuan Tran, and Khoi Nguyen. Dataset diffusion: Diffusion-based synthetic data generation for pixel-level semantic segmentation. In *NeurIPS*, 2023.
- [45] Maxime Oquab, Timothée Darcet, Théo Moutakanni, Huy Vo, Marc Szafraniec, Vasil Khalidov, Pierre Fernandez, Daniel Haziza, Francisco Massa, Alaaeldin El-Nouby, et al. Dinov2: Learning robust visual features without supervision. *arXiv preprint arXiv:2304.07193*, 2023.
- [46] Long Ouyang, Jeffrey Wu, Xu Jiang, Diogo Almeida, Carroll Wainwright, Pamela Mishkin, Chong Zhang, Sandhini Agarwal, Katarina Slama, Alex Ray, et al. Training language models to follow instructions with human feedback. In *NeurIPS*, 2022.
- [47] Jordi Pont-Tuset, Federico Perazzi, Sergi Caelles, Pablo Arbeláez, Alex Sorkine-Hornung, and Luc Van Gool. The 2017 davis challenge on video object segmentation. *arXiv preprint arXiv:1704.00675*, 2017.
- [48] Alec Radford, Karthik Narasimhan, Tim Salimans, Ilya Sutskever, et al. Improving language understanding by generative pre-training. *OpenAI blog*, 2018.
- [49] Alec Radford, Jeffrey Wu, Rewon Child, David Luan, Dario Amodei, Ilya Sutskever, et al. Language models are unsupervised multitask learners. *OpenAI blog*, 2019.
- [50] Alec Radford, Jong Wook Kim, Chris Hallacy, Aditya Ramesh, Gabriel Goh, Sandhini Agarwal, Girish Sastry, Amanda Askell, Pamela Mishkin, Jack Clark, et al. Learning transferable visual models from natural language supervision. In *ICML*, 2021.
- [51] Shaoqing Ren, Kaiming He, Ross Girshick, and Jian Sun. Faster r-cnn: Towards real-time object detection with region proposal networks. In *NeurIPS*, 2015.
- [52] Robin Rombach, Andreas Blattmann, Dominik Lorenz, Patrick Esser, and Björn Ommer. High-resolution image synthesis with latent diffusion models. In *CVPR*, 2022.
- [53] Carole H Sudre, Wenqi Li, Tom Vercauteren, Sebastien Ourselin, and M Jorge Cardoso. Generalised dice overlap as a deep learning loss function for highly unbalanced segmentations. In *Deep Learning in Medical Image Analysis and Multimodal Learning for Clinical Decision Support: Third International Workshop, DLMIA 2017, and 7th International Workshop, ML-CDS 2017, Held in Conjunction with MICCAI 2017, Québec City, QC, Canada, September 14, Proceedings 3*, 2017.
- [54] Matthew Tancik, Pratul Srinivasan, Ben Mildenhall, Sara Fridovich-Keil, Nithin Raghavan, Utkarsh Singhal, Ravi Ramamoorthi, Jonathan Barron, and Ren Ng. Fourier features let networks learn high frequency functions in low dimensional domains. In *NeurIPS*, 2020.
- [55] Luming Tang, Menglin Jia, Qianqian Wang, Cheng Perng Phoo, and Bharath Hariharan. Emergent correspondence from image diffusion. *arXiv preprint arXiv:2306.03881*, 2023.
- [56] Ashish Vaswani, Noam Shazeer, Niki Parmar, Jakob Uszkoreit, Llion Jones, Aidan N Gomez, Łukasz Kaiser, and Illia Polosukhin. Attention is all you need. In *NeurIPS*, 2017.
- [57] Xiaolong Wang, Allan Jabri, and Alexei A Efros. Learning correspondence from the cycle-consistency of time. In *CVPR*, pages 2566–2576, 2019.
- [58] Xinlong Wang, Wen Wang, Yue Cao, Chunhua Shen, and Tiejun Huang. Images speak in images: A generalist painter for in-context visual learning. In *painter*, 2023.
- [59] Xinlong Wang, Xiaosong Zhang, Yue Cao, Wen Wang, Chunhua Shen, and Tiejun Huang. Seggpt: Towards segmenting everything in context. In *CVPR*, 2023.
- [60] Tete Xiao, Yingcheng Liu, Bolei Zhou, Yuning Jiang, and Jian Sun. Unified perceptual parsing for scene understanding. In *ECCV*, 2018.
- [61] Sang Michael Xie, Aditi Raghunathan, Percy Liang, and Tengyu Ma. An explanation of in-context learning as implicit bayesian inference. In *ICLR*, 2021.

- [62] Ning Xu, Linjie Yang, Yuchen Fan, Dingcheng Yue, Yuchen Liang, Jianchao Yang, and Thomas Huang. Youtube-vos: A large-scale video object segmentation benchmark. *arXiv preprint arXiv:1809.03327*, 2018.
- [63] Bin Yan, Yi Jiang, Jiannan Wu, Dong Wang, Ping Luo, Zehuan Yuan, and Huchuan Lu. Universal instance perception as object discovery and retrieval. In *CVPR*, pages 15325–15336, 2023.
- [64] Jiahui Yu, Zirui Wang, Vijay Vasudevan, Legg Yeung, Mojtaba Seyedhosseini, and Yonghui Wu. Coca: Contrastive captioners are image-text foundation models. *arXiv preprint arXiv:2205.01917*, 2022.
- [65] Jian-Wei Zhang, Yifan Sun, Yi Yang, and Wei Chen. Feature-proxy transformer for few-shot segmentation. *Advances in Neural Information Processing Systems*, 2022.
- [66] Renrui Zhang, Zhengkai Jiang, Ziyu Guo, Shilin Yan, Junting Pan, Hao Dong, Peng Gao, and Hongsheng Li. Personalize segment anything model with one shot. *arXiv preprint arXiv:2305.03048*, 2023.
- [67] Bolei Zhou, Hang Zhao, Xavier Puig, Tete Xiao, Sanja Fidler, Adela Barriuso, and Antonio Torralba. Semantic understanding of scenes through the ade20k dataset. *IJCV*, 2019.
- [68] Xingyi Zhou, Vladlen Koltun, and Philipp Krähenbühl. Simple multi-dataset detection. In *CVPR*, 2022.
- [69] Xueyan Zou, Zi-Yi Dou, Jianwei Yang, Zhe Gan, Linjie Li, Chunyuan Li, Xiyang Dai, Harkirat Behl, Jianfeng Wang, Lu Yuan, et al. Generalized decoding for pixel, image, and language. In *CVPR*, 2023.
- [70] Xueyan Zou, Jianwei Yang, Hao Zhang, Feng Li, Linjie Li, Jianfeng Gao, and Yong Jae Lee. Segment everything everywhere all at once. In *NeurIPS*, 2023.